
ADAPTS: LIGHTWEIGHT TEACHER-STUDENT APPROACH FOR MULTI-CLASS AND CONTINUAL VISUAL ANOMALY DETECTION

Manuel Barusco
University of Padova, Italy
manuel.barusco@phd.unipd.it

Davide Dalle Pezze
University of Padova, Italy
davide.dallepezze@unipd.it

Francesco Borsatti
University of Padova, Italy
francesco.borsatti.1@phd.unipd.it

Gian Antonio Susto
University of Padova, Italy
gianantonio.susto@unipd.it

ABSTRACT

Visual Anomaly Detection (VAD) is crucial for industrial inspection, yet most existing methods are limited to single-category scenarios, failing to address the multi-class and continual learning demands of real-world environments. While Teacher-Student (TS) architectures are efficient, they remain unexplored for the Continual Setting. To bridge this gap, we propose AdapTS, a unified TS framework designed for multi-class and continual settings, optimized for edge deployment. AdapTS eliminates the need for two different architectures by utilizing a single shared frozen backbone and injecting lightweight trainable adapters into the student pathway. Training is enhanced via a segmentation-guided objective and synthetic Perlin noise, while a prototype-based task identification mechanism dynamically selects adapters at inference with 99% accuracy. Experiments on MVTec AD and VisA demonstrate that AdapTS matches the performance of existing TS methods across multi-class and continual learning scenarios, while drastically reducing memory overhead. Our lightest variant, AdapTS-S, requires only 8 MB of additional memory, 13x less than STFPM (95 MB), 48x less than RD4AD (360 MB), and 149x less than DeSTSeg (1120 MB), making it a highly scalable solution for edge deployment in complex industrial environments.

Keywords Visual Anomaly Detection · Multi-Class · Continual Learning

1 Introduction

VAD is a computer vision task that aims to identify anomalous images in industrial scenarios. Its key advantage lies in its unsupervised nature: models are trained exclusively on anomaly-free samples from a given category, eliminating the need for costly pixel-level annotations. In addition, VAD methods can localize anomalous regions at the pixel level, providing interpretable insights that support faster and more reliable decision-making.

While most VAD literature considers single-category models, the real industrial environments are much more complex. Modern inspection lines often process multiple product types simultaneously (Multi-Class Setting), while new products are continuously introduced over time (Continual Setting).

VAD methods fall into two broad categories. Reconstruction-based approaches operate directly in image space, reconstructing the input and flagging deviations as anomalies, but are computationally expensive. Feature-based approaches instead leverage pretrained encoders and can be further divided into memory-bank, normalizing flow, and teacher-student (TS) methods, generally offering a better efficiency-performance trade-off.

Despite its efficiency advantages, the TS framework remains entirely unexplored in the continual learning setting. Although hybrid approaches have been proposed for the multi-class scenario, none extend to continual learning, and no existing method simultaneously addresses both challenges within a single unified framework.

Therefore, we propose **AdapTS**, an approach based on the TS framework, which works inherently for both multi-class and continual settings with a focus on edge deployment. Rather than maintaining two separate networks, we propose to use a single pretrained backbone that simultaneously plays the role of both teacher and student. This is achieved by attaching small, trainable adapter modules to the student pathway, while keeping the underlying network weights frozen. To further improve localization accuracy, we augment the training procedure with a segmentation-guided objective and synthetic anomalies via Perlin noise. This encourages the adapters to produce feature discrepancies that are spatially coherent and semantically meaningful. Finally, to support multi-task scenarios, we introduce a prototype-based task identification mechanism that selects the appropriate set of adapters at inference time based on the similarity between the input image and per-task feature prototypes.

Our contributions are as follows:

- We propose AdapTS, a novel TS approach for VAD. We use a single pretrained backbone acting simultaneously as teacher and student, achieved by attaching small trainable adapter modules to the student pathway.
- Unlike existing TS methods, AdapTS is natively suited for both multi-class and continual learning settings.
- AdapTS achieves a significantly lower memory footprint compared to existing approaches, making it well-suited for deployment on edge devices with constrained resources.
- We conduct extensive experiments on the MVTec AD and VisA benchmarks, demonstrating that AdapTS achieves comparable performance to state-of-the-art TS methods while offering substantial memory savings across single, multi-task, and continual learning scenarios.

The remainder of this paper is structured as follows: Section 2 surveys the VAD literature, with particular emphasis on TS frameworks and related methodologies, as well as multiclass and continual learning settings. Section 3 introduces the proposed AdapTS framework, describing its adapter layers, segmentation-guided training strategy, and task identification mechanism. Section 4 outlines the experimental setup, including the benchmarks and evaluation metrics employed. Section 5 presents and analyzes results on the MVTec AD and VisA benchmarks across single-class, multi-class, and continual learning scenarios. Finally, Section 6 draws conclusions and outlines directions for future work.

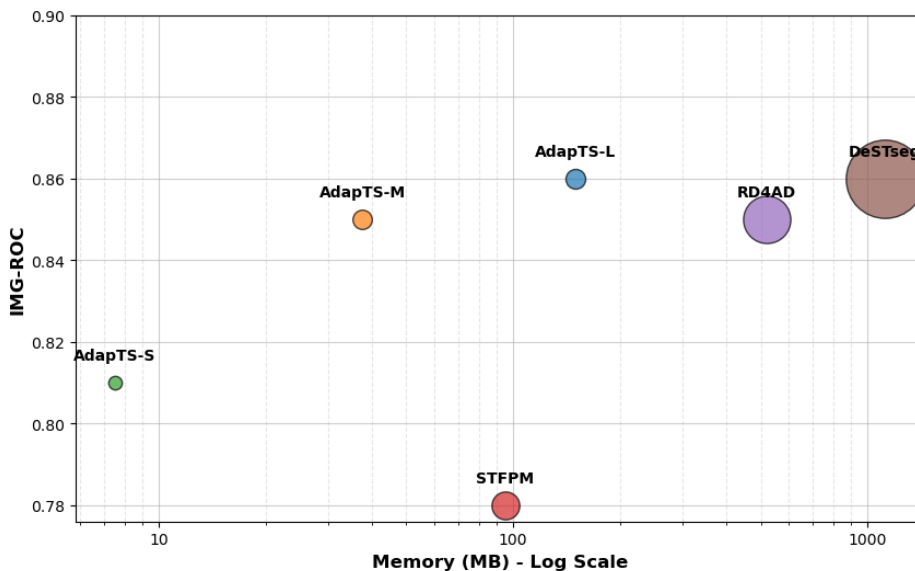


Figure 1: Comparison of the methods in terms of Image ROC on the MVTec dataset in the Multi-Class scenario, Model Memory (MB) required by each VAD method, and Inference VRAM peak represented by the size of the circles.

2 Related Work

2.1 Visual Anomaly Detection

VAD is a computer vision task aimed at identifying anomalous images. Its key advantages are its unsupervised nature, models train exclusively on anomaly-free samples, eliminating costly pixel-level annotations, and the ability to localize anomalous regions at the pixel level, offering interpretable insights for faster decision-making. While most commonly applied to industrial quality control, VAD also extends to medical imaging and remote sensing [1].

Early approaches relied on **reconstruction-based** methods (autoencoders or [2]), which are computationally expensive and often underperform. The current trend favors **feature-based** VAD, which leverages pretrained models for higher performance at lower computational cost.

Feature-based methods fall into three categories: memory-bank methods (e.g., PatchCore [3], PaDiM [4], CFA [5]), which store representative patch-level embeddings; normalizing flow methods (eg. FastFlow [6]), which model the normal feature distribution but tend to be computationally intensive; and teacher-student methods, which use the feature discrepancy between a frozen teacher and a trainable student as the anomaly signal.

2.2 Teacher-Student Methods

The student-teacher framework leverages knowledge distillation to identify anomalies. The core principle is that a student trained only on normal samples produces features that diverge from those of a pre-trained teacher when anomalous inputs are encountered.

STFPM [7] transfers knowledge from a frozen, pretrained teacher network to a randomly initialized student that shares the same architecture. During training on normal images only, the student learns to replicate the teacher’s feature representations. At inference, the model compares their multi-scale feature maps hierarchically to identify deviations that signal anomalies. This hierarchical matching strategy delivers meaningful gains in accuracy.

Beyond STFPM, hybrid approaches combine reconstruction-based methods with the teacher-student (TS) framework, so in the following text, we refer to them as both TS and hybrid approaches. They adopt an encoder-decoder architecture and like the TS framework, they employ a frozen encoder and detect anomalies by comparing feature maps produced by the encoder and the decoder, rather than computing differences at the image level as in classic reconstruction-based approaches. While they are computationally less expensive than reconstruction-based models, they are more heavy than the original STFPM (see Table 1).

Reverse Distillation (RD4AD) follows this encoder-decoder framework [8]. The student receives a compact bottleneck embedding and reconstructs the teacher’s multi-scale representations, naturally suppressing anomalous perturbations through reverse knowledge flow.

Another example is DeSTSeg, which extends the paradigm with a denoising training procedure and a learnable segmentation network [9]. The student network is trained to reconstruct the teacher’s clean features from synthetically corrupted images, while a segmentation network fuses multi-level discrepancies using synthetic anomaly masks as supervision.

2.3 Multi-Class and Continual Learning Settings

Traditional VAD systems follow a “one-category-one-model” assumption: a dedicated model is trained on normal samples from a single product category and deployed exclusively for it. While effective, this is incompatible with modern industrial production, where dozens of product types may share a single inspection line (multi-class setting) and new products arrive over time (continual setting). In addition, the cost of training and maintaining a separate model quickly becomes prohibitive.

Multi-class Setting requires a single unified model to distinguish normal from anomalous samples across multiple categories simultaneously, without prior knowledge of the category to which a test image belongs. This setting demands a feature space that is sufficiently expressive to capture diverse normal patterns without mixing them, while also accommodating semantically varied anomaly types across categories.

Several methods address this setting. [10] proposes a reconstruction-based approach using diffusion models, though at high computational cost due to operating in image space. Hybrid approaches extending RD4AD have also been proposed [11, 12], which are more efficient than pure reconstruction-based approaches, as the encoder remains frozen during training. Building on its encoder-decoder architecture, these approaches keep the CNN pretrained encoder but substitute the CNN-based decoder with transformer-based and Mamba-based variants, respectively. While more efficient than pure reconstruction methods, they remain more expensive to train and store than the original STFPM.

It should be noted that while they were not originally designed for that, STFPM, RD4AD, DeSTseg can easily operate in the multi-class setting. In fact, RD4AD shows comparable performance to models specifically designed for multi-class, like [11].

Continual Learning assumes categories are introduced sequentially as a stream of tasks, requiring adaptation to new data while preserving prior knowledge, inheriting the challenges of Multi-Class learning with the added difficulty of an evolving data distribution and the impossibility to access previous data distributions when training on a new category.

Early work applied standard CL strategies such as Replay to VAD [13]. Replay mitigates catastrophic forgetting by interleaving past and new data during training using a replay buffer: an additional memory where a small fraction of past data is stored.

Building on this, researchers have proposed various methods designed specifically to tackle VAD within the CL paradigm, including memory-bank approaches [14, 15, 16] and reconstruction-based methods [17, 18, 19].

Notably, hybrid approaches proposed for the multi-class setting do not address continual learning, and existing CL methods have overlooked the TS framework entirely. To the best of our knowledge, no TS method simultaneously addresses both settings. To fill this gap, we propose AdapTS, an extension of STFPM that natively handles both settings within a unified architecture, achieving competitive detection performance at a fraction of the memory footprint of TS and, more generally, of the VAD approaches.

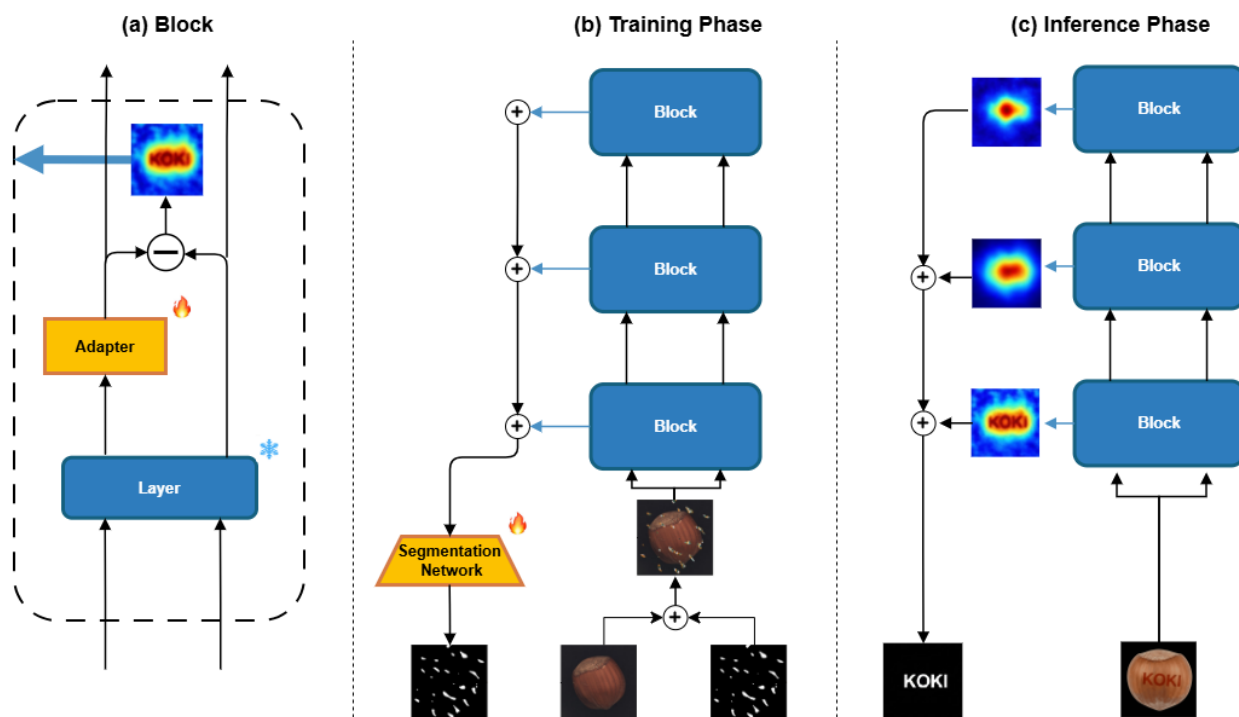


Figure 2: Overview of **AdapTS architecture**. (a) Main Block of the method with frozen weights (blue blocks), trainable weights (yellow blocks), and difference feature maps output (blue arrow). (b) During training, synthetic anomalies are introduced alongside a segmentation network to guide learning and separability. (c) In the inference phase, the segmentation network is discarded for efficient anomaly detection.

3 Method

Since our method builds on the STFPM framework, we describe it in detail in Section 3.1. Then we discuss the change of the original dual-network student-teacher paradigm in Section 3.2. To improve performance and regularize the training, we propose an additional segmentation loss described in Section 3.3. Eventually, to handle the multi-task and continual learning scenarios, we propose a simple solution described in Section 3.4.

3.1 Student-Teacher Feature Pyramid Matching for Anomaly Detection

The Student-Teacher Feature Pyramid Matching (STFPM) model identifies visual defects using a student network S and a teacher network T , both sharing the same architecture. The student, initialized randomly, is trained to replicate

the frozen ImageNet-pretrained teacher’s multi-scale feature representations on normal images. Given a training dataset of normal images $D = \{x_1, \dots, x_n\}$, for every input image $x_i \in \mathbb{R}^{W \times H \times C}$, we extract the intermediate feature maps $\{F_T^l(x)\}_{l \in L}$ from the teacher T and $\{F_S^l(x)\}_{l \in L}$ from the student S , across a set of selected layers L . $F_T^l(x), F_S^l(x) \in \mathbb{R}^{W_l \times H_l \times C_l}$ where H_l and W_l denote the spatial dimensions at layer l .

The student is trained to mimic the teacher by minimizing a feature-wise discrepancy loss:

$$\mathcal{L}_{\text{STFPM}} = \sum_{l \in L} \frac{1}{H_l W_l} \|\phi(F_T^l(x)) - \phi(F_S^l(x))\|_2^2, \quad (1)$$

where $\phi(\cdot)$ represents channel-wise normalization. The teacher remains frozen during training, while only the student parameters are updated.

At inference time, the anomaly heatmaps are produced by calculating the differences between the feature maps extracted by S and T , upsampled to the input image resolution.

3.2 Proposed Approach

By introducing the TS framework, STFPM established a promising research direction, but the original framework remains fundamentally inefficient. Instead, we propose a more parameter-efficient alternative called AdapTS; rather than training a separate student, we augment the teacher itself by inserting lightweight adapter layers directly into its architecture.

These adapters are trained with the same STFPM’s objective: to reconstruct the teacher’s own intermediate features, transforming the augmented teacher into its own student. In addition, this design reduces the number of additional parameters to a small fraction of those required by STFPM, which relies on a fully randomly initialized copy of the teacher architecture.

The adapters are attached to the output feature maps of the teacher feature-extraction layers, process them, and pass them through the rest of the network. The adapters create a discrepancy between the student and teacher behaviors, which is minimized during adapter training on normal images using the $\mathcal{L}_{\text{STFPM}}$ loss. The adapters are trainable while the teacher pretrained network remains frozen. Different adapter architectures have been considered and are listed below.

To formalize the behavior of the developed adapters, we first define the following common notations:

- $\mathbf{x} \in \mathbb{R}^{C \times H \times W}$ is the input tensor, where C is the number of channels and H, W are the spatial dimensions.
- The symbol $*$ denotes the spatial convolution operator with a 1×1 kernel.
- $\mathbf{W}_1 \in \mathbb{R}^{C_{\text{latent}} \times C \times 1 \times 1}$, \mathbf{b}_1 and $\mathbf{W}_2 \in \mathbb{R}^{C \times C_{\text{latent}} \times 1 \times 1}$, \mathbf{b}_2 represent the weights and biases of the first and second convolutions, respectively.
- $\text{BN}(\cdot)$ represents the spatial Batch Normalization operation.
- $\sigma(\cdot)$ is the ReLU activation function, defined as $\sigma(z) = \max(0, z)$.

All adapters share a unified residual architecture governed by a single equation, where the input \mathbf{x} is added to the output of two sequential 1×1 convolutions with an intermediate Batch Normalization and non-linearity:

$$\mathbf{y} = \mathbf{x} + \mathbf{W}_2 * \sigma\left(\text{BN}(\mathbf{W}_1 * \mathbf{x} + \mathbf{b}_1)\right) + \mathbf{b}_2 \quad (2)$$

The three adapter variants differ solely in the choice of the latent dimensionality C_{latent} :

- **Linear adapter:** $C_{\text{latent}} = C$. The channel dimension is preserved throughout, so both projection matrices are square.
- **Expansion adapter:** $C_{\text{latent}} = C \cdot E$, with expansion factor $E > 1$. Features are projected into a higher-dimensional space to improve intermediate separability between student and teacher representations, before being projected back.
- **Bottleneck adapter:** $C_{\text{latent}} = \max(1, \lfloor C \cdot R \rfloor)$, with reduction factor $0 < R < 1$. Features are compressed into a lower-dimensional bottleneck to encourage the adapter to focus on reproducing only the most informative teacher features, suppressing spurious noise. We analyze two bottleneck variants, BN25 and BN50, with reduction factors $E = 0.25$ and $E = 0.5$, respectively.

To further reduce the memory footprint of AdapTS, the adapters can be INT-8 quantized using a post-training quantization procedure without heavily impacting the performance as demonstrated in Table 1 and as discussed in Sec. 5.2.

3.3 Segmentation guided training

To improve adapters training and performance, a segmentation-guided training similar to [9] has been developed. During training, the differences between the student and teacher feature maps at different feature-extraction layers are upsampled in order to match their spatial dimensions, concatenated channel-wise, and fed into a simple segmentation network to produce the final anomaly segmentation map.

Since in a typical VAD scenario the training set consists only of normal images, synthetic anomalies (generated with Perlin noise combined with random textures as in [9]) have been added to the normal dataset to produce anomalous images and their corresponding segmentation masks. The segmentation network consists of a 1×1 convolutional layer that projects the multi-channel input into a single channel, followed by a sigmoid activation to generate a spatial, pixel-wise probability map.

Compared to [9], we utilize a significantly simpler segmentation network. If we used a high-capacity network, it could easily detect anomalies by leveraging complex data patterns in the input feature differences, effectively masking poor alignment between student and teacher. Our simple design avoids this pitfall, forcing a better inherent separability between normal and anomalous features. Because the segmentation head is discarded post-training, the final performance relies entirely on the improved quality of these raw feature differences. The segmentation head is trained jointly with the adapters using a combined loss function comprising Focal Loss and L1 Loss.

$$\mathcal{L}_{focal} = -\frac{1}{H_s W_s} \sum_{i,j=1}^{H_s, W_s} (1 - p_{ij})^\gamma \log(p_{ij}), \quad \mathcal{L}_{l1} = \frac{1}{H_s W_s} \sum_{i,j=1}^{H_s, W_s} |M_{ij} - \hat{Y}_{ij}| \quad (3)$$

$$\mathcal{L}_{seg} = \mathcal{L}_{focal} + \mathcal{L}_{l1} \quad (4)$$

The ground-truth anomaly mask is downsampled to match the output size (H_s, W_s) . Denoting the predicted probability map as \hat{Y} and the downsampled mask as M , the focal loss is computed with $p_{ij} = M_{ij}\hat{Y}_{ij} + (1 - M_{ij})(1 - \hat{Y}_{ij})$, where γ is the focusing parameter. The focal loss help the model to focus on the minority category and difficult samples while the L1 loss is employed to improve the sparsity of the output so that the segmentation mask’s boundaries are more distinct. After the training, the segmentation head is discarded, and only the adapters are used for the inference. The final loss for training the adapters is thus:

$$\mathcal{L} = \mathcal{L}_{STFPM} + \mathcal{L}_{seg} \quad (5)$$

Figure 2 visually summarize the key components of AdapTS.

3.4 Task identification

A key advantage of our approach is the ability to train task-specific adapters tailored to different input data distributions. Let $\mathcal{T} = \{1, \dots, K\}$ denote the set of tasks (anomalous objects or categories in the dataset). For each task $t \in \mathcal{T}$, we define a prototype $\mathbf{p}_t \in \mathbb{R}^D$ computed from features extracted by the pretrained teacher $T(\cdot)$, immediately before the classification head.

Given the training set $\mathcal{D}_t = \{x_i^{(t)}\}_{i=1}^{N_t}$ for task t , the prototype is defined as

$$\mathbf{p}_t = \frac{1}{N_t} \sum_{i=1}^{N_t} T(x_i^{(t)}).$$

At inference time, for a test image x , we compute its feature representation $\mathbf{z} = T(x) \in \mathbb{R}^C$ and assign the task label according to a similarity function (in our case the Euclidean distance) $s(\cdot, \cdot)$:

$$\hat{k} = \arg \max_{t \in \mathcal{T}} s(\mathbf{z}, \mathbf{p}_t),$$

thus selecting the adapter associated with the most similar task prototype. This procedure can adapt our method to the continual learning and multi-class scenarios.

4 Experimental Setting

4.1 Implementation Details

All the VAD models are tested using the WideResnet50_2 model pretrained on the ImageNet dataset as a teacher feature extractor. All experiments have been conducted on a workstation with an AMD Ryzen Threadripper PRO

5995WX CPU and an NVIDIA RTX A6000 GPU. The AdapTS source code is publicly available ¹; the other VAD models have been tested using their officially published code.

4.2 Datasets

The datasets considered in the experiments are MVTec and VisA, the two main benchmarks for Visual Anomaly Detection. MVTec AD [20] contains high-resolution images across 15 categories (10 objects and 5 textures), with a defect-free training set and a test set including both normal and anomalous samples with pixel-level annotations. VisA [21] comprises 10,821 high-resolution color images across 12 objects in 3 domains.

4.3 Models

We evaluated three variants of our proposed method against state-of-the-art VAD models built on the Teacher-Student framework. The comparison includes the following approaches:

- **AdapTS-L**: Our method with adapters applied at layers 2 and 3.
- **AdapTS-M**: AdapTS-L with INT-8 quantized adapters at layers 2 and 3.
- **AdapTS-S**: Our lightest variant, using only the INT-8 quantized adapter at layer 2.
- **STFPM, RD4AD, DeSTSeG** : Described in Section 3.1 and Section 2.

While our primary focus is the comparison of VAD approaches within the TS framework, we also present a broader evaluation that includes several state-of-the-art VAD methods on the VisA Dataset (see Tab. 2). Specifically, we evaluate a well-known feature-based method (SimpleNet [22]) and a reconstruction-based approach (DiAD [10]). Additionally, we compare AdapTS with the results reported in the original paper by the authors of MambaAD [12], which builds on RD4AD but employs a Mamba-based model as the decoder. For a fair comparison, we report the results obtained using the same encoder as ours, WideResNet50.

4.4 Scenarios

All the considered VAD models are tested on three different scenarios:

- **Single Models**: A different model is trained for every dataset category.
- **Multi Class**: A single model is trained for all the categories.
- **Continual**: A single model is trained sequentially on the stream of categories.

As discussed in Section 3.4, our solution is inherently designed to support both Multi-Class and Continual learning scenarios. In contrast, STFPM, RD4AD, and DeSTSeg are not natively suited for the Continual setting. To enable a fair comparison, we apply a Replay strategy to adapt these methods. Specifically, we use a replay buffer of 100 samples, which has a similar memory footprint compared to our adapters.

4.5 Evaluation Metrics

We evaluate all methods using standard VAD metrics:

- **I-ROC and P-ROC**: AUROC computed at the image and pixel level, respectively.
- **P-F1**: Harmonic mean of Precision and Recall at pixel level.
- **AP**: Area under the Precision-Recall curve at pixel level.
- **Additional Memory**: Memory needed for all model components except the teacher, e.g., the student network in STFPM or the replay buffer required in the continual setting by all compared approaches.
- **Memory Footprint**: Total model memory comprising the pretrained teacher network plus any additional memory.
- **VRAM and FLOPs**: We measure for both inference and training the VRAM occupied and the FLOPs required.

In the *Multi-Class* setting, each metric is computed independently per category and averaged. In the *Continual Learning* setting, metrics are computed after sequential training on all categories and averaged.

¹AdapTS github repository <https://github.com/groupvad/adapts>

Table 1: Comparison of anomaly detection models. **Bold** indicates the best result per scenario. Inf: Inference, Tr Training, Tot: Total, Add: Additional.

Scenario	Model	Image		Pixel		Mem (MB)		FLOPs (G)		VRAM (MB)	
		I-ROC	P-ROC	P-F1	AP	Tot	Add	Inf	Tr	Inf	Tr
Single	AdapTS-L	0.88	0.94	0.50	0.46	105	10	44	90	169	358
	AdapTS-M	0.86	0.94	0.49	0.46	97	3	44	90	161	350
	AdapTS-S	0.82	0.91	0.40	0.37	16	1	34	69	80	172
	STFPM	0.88	0.96	0.54	0.51	190	95	37	74	335	604
	RD4AD	0.97	0.97	0.60	0.58	615	360	48	147	970	1242
	DeSTseg	0.98	0.98	0.67	0.75	1215	1120	187	977	2646	3241
Multi-Class	AdapTS-L	0.86	0.94	0.50	0.44	245	150	44	90	169	358
	AdapTS-M	0.85	0.93	0.49	0.46	132	38	44	90	161	351
	AdapTS-S	0.81	0.90	0.41	0.37	23	8	35	69	80	172
	STFPM	0.78	0.95	0.45	0.44	190	95	37	74	335	604
	RD4AD	0.85	0.93	0.48	0.41	615	360	48	147	970	1242
	DeSTseg	0.86	0.92	0.54	0.55	1215	1120	187	977	2646	3241
Continual	AdapTS-L	0.86	0.94	0.50	0.44	245	150	44	90	169	358
	AdapTS-M	0.85	0.93	0.49	0.46	132	38	44	90	161	351
	AdapTS-S	0.81	0.90	0.41	0.37	23	8	34	69	80	172
	STFPM	0.78	0.91	0.41	0.36	204	110	37	74	335	604
	RD4AD	0.94	0.95	0.51	0.47	629	374	48	147	970	1242
	DeSTseg	0.80	0.92	0.46	0.45	1229	1134	187	977	2646	3241

5 Results

5.1 Performance Comparison among the settings

Table 1 reports the comparison between AdapTS variants (L/M/S) and TS approaches on MVTEC under three settings: Single, Multi-Class, Continual.

In the **Single setting**, DeSTSeg achieves the best detection performance, followed by RD4AD, but at a high memory cost (1215 and 615 MB). AdapTS offers a more efficient alternative: by sharing a single backbone between teacher and student and training only lightweight adapters, it reduces memory to just 105, 97, and 16 MB for the L, M, and S variants respectively, compared to 615 MB of STFPM, while achieving comparable accuracy.

In the **Multi-Class scenario**, DeSTSeg remains the top performer but is computationally heavy. AdapTS-M matches RD4AD and outperforms STFPM with substantially less memory, confirming the scalability of our approach. A visual comparison of the performance-memory tradeoff across all the considered VAD models in the Multi-Class scenario on the MVTEC Dataset is visible in Figure 1. Some examples of Anomaly Detection results produced by AdapTS on the MVTEC Dataset are visible in Figure 3.

In the **Continual scenario**, AdapTS reaches similar values to STFPM and DeSTSeg for most of the metrics while maintaining a dramatically lower memory footprint.

Table 2: Comparison of anomaly detection models in the Multi-Class scenario on the VisA dataset. **Bold** values indicate the best result per metric, computed separately for the top and bottom sections. Add: Additional Memory, Total: backbone and Additional Memory.

Model	Image-level	Pixel-level			Memory (MB)	
	I-ROC	P-ROC	P-F1	AP	Total	Add
AdapTS-L (our)	0.83	0.96	0.35	0.27	245	150
AdapTS-M (our)	0.82	0.96	0.34	0.26	132	37
AdapTS-S (our)	0.79	0.93	0.33	0.25	23	7
STFPM (BMVC 2021)	0.79	0.95	0.36	0.23	190	95
RD4AD (CVPR 2022)	0.85	0.93	0.37	0.26	615	360
DeSTSeg (CVPR 2023)	0.87	0.96	0.47	0.41	1,215	1,120
SimpleNet (CVPR 2023)	0.87	0.97	0.38	0.35	291.0	–
DiAD (AAAI 2024)	0.87	0.96	0.33	0.26	5325.0	–
MambaAD (NeurIPS 2024)	0.98	0.99	0.60	0.58	1072.0	–

Table 3: Performance comparison of different adapter architectures attached to layers 1, 2, and 3 on the MVTec dataset. **Bold** values indicate the best result per metric.

Model	Image-level	Pixel-level			Memory [MB]	
	I-ROC	P-ROC	P-F1	AP	Normal	Quantized
Linear	0.86	0.93	0.46	0.44	10.54	2.64
BN25	0.77	0.89	0.32	0.26	2.67	0.68
BN50	0.78	0.90	0.35	0.30	5.30	1.33
Expansion	0.87	0.94	0.46	0.43	21.07	5.28
Linear Seg	0.87	0.94	0.49	0.45	10.54	2.64

5.2 Ablation Studies

As discussed in Section 3.2, Table 3 compares four adapter configurations. BN25 and BN50 perform poorly, as aggressive feature compression degrades representation quality. The Linear configuration achieves the best performance, while Expansion fails to justify its doubled parameter count with respect to the gains obtained, confirming that increasing dimensionality yields diminishing returns beyond a certain point.

Linear Seg, which combines linear adapters with the segmentation network, achieves the best overall performance with gains on pixel-level metrics. Table 4 studies the effect of placing adapters across the teacher layers. Layers 2 and 3 (AdapTS-M and AdapTS-L) yield the best performance, while the single-layer Layer 2 variant (AdapTS-S) remains competitive, suggesting Layer 2 features are particularly informative for VAD.

Notably, when examining the variant AdapTS-M, where the adapters of AdapTS-L are quantized, it has a negligible impact on performance: most metrics remain invariant, and I-ROC decreases marginally from 0.88 to 0.86, while delivering a substantial reduction in the additional memory. In addition, by removing the Layer 3 adapter, the additional memory is reduced by 4×, and since the last backbone layer is no longer needed, it can be discarded entirely, further reducing the total memory footprint.

Eventually, the task identification mechanism achieves 99% accuracy on both MVTec and VisA, showing that anomaly categories are linearly separable and no complex identification strategy is needed.

5.3 VisA Dataset

Table 2 shows the performance–efficiency trade-off in the Multi-Class scenario on VisA. Top-performing methods like MambaAD (I-ROC: 0.98, 1,072 MB), SimpleNet (I-ROC: 0.87, 291 MB), and DiAD (I-ROC: 0.87, 5,325 MB) prioritize accuracy regardless of memory cost, making them unsuitable for resource-constrained deployment.

AdapTS targets a different regime. AdapTS-L achieves I-ROC 0.83 and matches DeSTSeg and DiAD on P-ROC (0.96) with only 245 MB total memory. AdapTS-M and AdapTS-S further reduce additional memory to 132 MB and 23

Table 4: Performance comparison when applying adapters to different feature extraction layer combinations using LinearSeg Adapters on the MVTec dataset. **Bold** values indicate the best result per metric.

Layers	Image-level	Pixel-level			Memory [MB]	
	I-ROC	P-ROC	P-F1	AP	Normal	Quantized
1-2-3	0.87	0.94	0.49	0.45	10.54	2.64
1-2	0.78	0.90	0.36	0.30	2.51	0.63
2-3	0.88	0.94	0.50	0.46	10.03	2.51
2	0.82	0.91	0.40	0.37	2.01	0.50

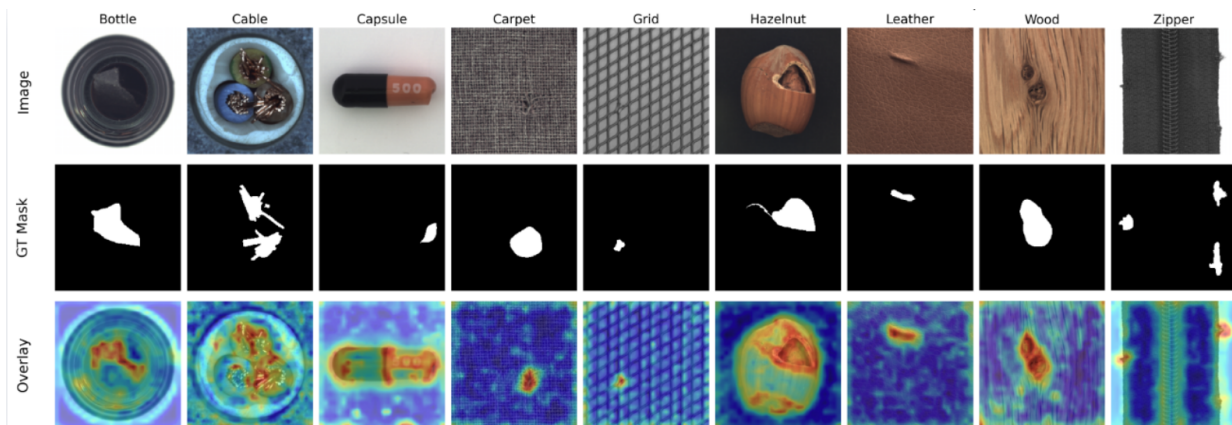


Figure 3: AdapTS anomaly detection examples on the MVTec Dataset. The first row contains an anomalous image per category, the second row the ground-truth anomaly mask and the third row the anomaly heatmap produced by AdapTS.

MB, respectively, the latter representing 46× savings over MambaAD. Within the TS family, AdapTS-L outperforms STFP (I-ROC 0.83 vs. 0.79) while halving its memory and remains competitive with RD4AD at less than half the memory cost (245 MB vs. 615 MB).

These results reinforce the claim that AdapTS can achieve competitive multi-class anomaly detection results without the memory overhead that characterizes state-of-the-art methods, making AdapTS a uniquely practical solution for real-world industrial deployment.

6 Conclusion

In this paper, we presented AdapTS, a lightweight and efficient VAD model built on top of the STFP architecture that can natively operate in the Multi-Task and Continual scenarios. Experiments on the MVTec AD and VisA benchmarks consistently demonstrate the favorable trade-off offered by AdapTS. While methods such as MambaAD, DeSTSeg, and RD4AD achieve higher absolute performance, they do so at memory costs orders of magnitude higher, making them impractical.

In contrast, AdapTS relies on a single shared frozen backbone augmented by lightweight trainable adapters. AdapTS achieves a dramatic reduction in memory footprint while preserving competitive anomaly detection performance.

AdapTS addresses a significant gap in the VAD literature as the first TS-based method to unify multi-class and continual learning within a single framework by using adapter layers. We hope this work encourages further exploration of parameter-efficient architectures in industrial inspection settings, where scalability and adaptability to evolving product distributions are essential requirements.

A natural extension of this work is to explore new parameter-efficient training strategies and combination strategies, such as model weight merging, to further reduce memory overhead while preserving performance.

References

- [1] Hai Ling, Jia Guo, Zhulin Tao, Yunkang Cao, Donglin Di, Hongyan Xu, Xiu Su, Yang Song, and Lei Fan. Adnet: A large-scale and extensible multi-domain benchmark for anomaly detection across 380 real-world categories. *arXiv preprint arXiv:2511.20169*, 2025.
- [2] Samet Akcay, Amir Atapour-Abarghouei, and Toby P Breckon. Ganomaly: Semi-supervised anomaly detection via adversarial training. In *Computer Vision—ACCV 2018: 14th Asian Conference on Computer Vision, Perth, Australia, December 2–6, 2018, Revised Selected Papers, Part III 14*, pages 622–637. Springer, 2019.
- [3] Karsten Roth, Latha Pemula, Joaquin Zepeda, Bernhard Schölkopf, Thomas Brox, and Peter Gehler. Towards total recall in industrial anomaly detection. *arXiv:2106.08265*, 2022.
- [4] Thomas Defard, Aleksandr Setkov, Angelique Loesch, and Romaric Audigier. PaDiM: A patch distribution modeling framework for anomaly detection and localization. In *Pattern Recognition. ICPR International Workshops and Challenges*, pages 475–489. Springer International Publishing, 2021.
- [5] Sungwook Lee, Seunghyun Lee, and Byung Cheol Song. Cfa: Coupled-hypersphere-based feature adaptation for target-oriented anomaly localization. *IEEE Access*, 10:78446–78454, 2022.
- [6] Jiawei Yu, Ye Zheng, Xiang Wang, Wei Li, Yushuang Wu, Rui Zhao, and Liwei Wu. Fastflow: Unsupervised anomaly detection and localization via 2d normalizing flows. *arXiv preprint arXiv:2111.07677*, 2021.
- [7] Guodong Wang, Shumin Han, Errui Ding, and Di Huang. Student-teacher feature pyramid matching for anomaly detection, 2021.
- [8] Hanqiu Deng and Xingyu Li. Anomaly detection via reverse distillation from one-class embedding. In *Proceedings of the IEEE/CVF conference on computer vision and pattern recognition*, pages 9737–9746, 2022.
- [9] Xuan Zhang, Shiyu Li, Xi Li, Ping Huang, Jiulong Shan, and Ting Chen. Destseg: Segmentation guided denoising student-teacher for anomaly detection. In *Proceedings of the IEEE/CVF conference on computer vision and pattern recognition*, pages 3914–3923, 2023.
- [10] Haoyang He, Jiangning Zhang, Hongxu Chen, Xuhai Chen, Zhishan Li, Xu Chen, Yabiao Wang, Chengjie Wang, and Lei Xie. A diffusion-based framework for multi-class anomaly detection. In *Proceedings of the AAAI conference on artificial intelligence*, volume 38, pages 8472–8480, 2024.
- [11] Zhiyuan You, Lei Cui, Yujun Shen, Kai Yang, Xin Lu, Yu Zheng, and Xinyi Le. A unified model for multi-class anomaly detection. *Advances in Neural Information Processing Systems*, 35:4571–4584, 2022.
- [12] Haoyang He, Yuhu Bai, Jiangning Zhang, Qingdong He, Hongxu Chen, Zhenye Gan, Chengjie Wang, Xiangtai Li, Guanzhong Tian, and Lei Xie. Mambaad: Exploring state space models for multi-class unsupervised anomaly detection. *Advances in Neural Information Processing Systems*, 37:71162–71187, 2024.
- [13] Nikola Bugarin, Jovana Bugarcic, Manuel Barusco, Davide Dalle Pezze, and Gian Antonio Susto. Unveiling the anomalies in an ever-changing world: A benchmark for pixel-level anomaly detection in continual learning. In *Proceedings of the IEEE/CVF conference on computer vision and pattern recognition*, pages 4065–4074, 2024.
- [14] Manuel Barusco, Francesco Borsatti, Nicola Beda, Davide Dalle Pezze, and Gian Antonio Susto. Towards continual visual anomaly detection in the medical domain. In *Proceedings of the International Workshop on Personalized Incremental Learning in Medicine*, pages 18–24, 2025.
- [15] Wujin Li, Jiawei Zhan, Jinbao Wang, Bizhong Xia, Bin-Bin Gao, Jun Liu, Chengjie Wang, and Feng Zheng. Towards continual adaptation in industrial anomaly detection. In *Proceedings of the 30th ACM International Conference on Multimedia*, pages 2871–2880, 2022.
- [16] Jiaqi Liu, Kai Wu, Qiang Nie, Ying Chen, Bin-Bin Gao, Yong Liu, Jinbao Wang, Chengjie Wang, and Feng Zheng. Unsupervised continual anomaly detection with contrastively-learned prompt. In *Proceedings of the AAAI conference on artificial intelligence*, volume 38, pages 3639–3647, 2024.
- [17] Xiaofan Li, Xin Tan, Zhuo Chen, Zhizhong Zhang, Ruixin Zhang, Rizen Guo, Guanna Jiang, Yulong Chen, Yanyun Qu, Lizhuang Ma, et al. One-for-more: Continual diffusion model for anomaly detection. In *Proceedings of the Computer Vision and Pattern Recognition Conference*, pages 4766–4775, 2025.
- [18] Davide Dalle Pezze, Eugenia Anello, Chiara Masiero, and Gian Antonio Susto. Continual learning approaches for anomaly detection. *Evolving Systems*, 16(4):111, 2025.
- [19] Jiaqi Tang, Hao Lu, Xiaogang Xu, Ruizheng Wu, Sixing Hu, Tong Zhang, Tsz Wa Cheng, Ming Ge, Ying-Cong Chen, and Fugee Tsung. An incremental unified framework for small defect inspection. In *European conference on computer vision*, pages 307–324. Springer, 2024.

- [20] Paul Bergmann, Michael Fauser, David Sattlegger, and Carsten Steger. Mvtec ad—a comprehensive real-world dataset for unsupervised anomaly detection. In *Proceedings of the IEEE/CVF conference on computer vision and pattern recognition*, pages 9592–9600, 2019.
- [21] Yang Zou, Jongheon Jeong, Latha Pemula, Dongqing Zhang, and Onkar Dabeer. Spot-the-difference self-supervised pre-training for anomaly detection and segmentation, 2022.
- [22] Zhikang Liu, Yiming Zhou, Yuansheng Xu, and Zilei Wang. Simplenet: A simple network for image anomaly detection and localization. In *Proceedings of the IEEE/CVF conference on computer vision and pattern recognition*, pages 20402–20411, 2023.